

See discussions, stats, and author profiles for this publication at: <https://www.researchgate.net/publication/265018781>

iTRAQ Quantitative Clinical Proteomics Revealed Role of Na⁺K⁺-ATPase and Its Correlation with Deamidation in Vascular Dementia

ARTICLE *in* JOURNAL OF PROTEOME RESEARCH · AUGUST 2014

Impact Factor: 4.25 · DOI: 10.1021/pr500754j · Source: PubMed

CITATIONS

4

READS

35

7 AUTHORS, INCLUDING:



[Sunil S Adav](#)

Nanyang Technological University

72 PUBLICATIONS 1,890 CITATIONS

[SEE PROFILE](#)



[Christopher L H Chen](#)

National University of Singapore

324 PUBLICATIONS 3,019 CITATIONS

[SEE PROFILE](#)

iTRAQ Quantitative Clinical Proteomics Revealed Role of Na⁺K⁺-ATPase and Its Correlation with Deamidation in Vascular Dementia

Sunil S. Adav,[†] Jingru Qian,[†] Yi Lin Ang,[†] Raj N. Kalaria,[‡] Mitchell K. P. Lai,^{§,||} Christopher P. Chen,^{§,||} and Siu Kwan Sze*,[†]

[†]School of Biological Sciences, Nanyang Technological University, 60 Nanyang Drive, Singapore 637551, Singapore

[‡]Institute for Ageing and Health, NIHR Biomedical Research Building, Newcastle University, Campus for Ageing and Vitality, Newcastle upon Tyne NE4 5PL, United Kingdom

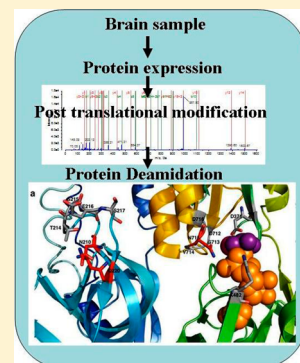
[§]Department of Pharmacology, Yong Loo Lin School of Medicine, National University of Singapore, 21 Lower Kent Ridge Road, Singapore 119077, Singapore

^{||}Memory, Aging and Cognition Centre, National University Health System, 18 Medical Drive, Singapore 117601, Singapore

Supporting Information

ABSTRACT: Dementia is a major public health burden characterized by impaired cognition and loss of function. There are limited treatment options due to inadequate understanding of its pathophysiology and underlying causative mechanisms. Discovery-driven iTRAQ-based quantitative proteomics techniques were applied on frozen brain samples to profile the proteome from vascular dementia (VaD) and age-matched nondementia controls to elucidate the perturbed pathways contributing to pathophysiology of VaD. The iTRAQ quantitative data revealed significant up-regulation of protein-L-isoaspartate O-methyltransferase and sodium–potassium transporting ATPase, while post-translational modification analysis suggested deamidation of catalytic and regulatory subunits of sodium–potassium transporting ATPase. Spontaneous protein deamidation of labile asparagines, generating abnormal L-isoaspartyl residues, is associated with cell aging and dementia due to Alzheimer's disease and may be a cause of neurodegeneration. As ion channel proteins play important roles in cellular signaling processes, alterations in their function by deamidation may lead to perturbations in membrane excitability and neuronal function. Structural modeling of sodium–potassium transporting ATPase revealed the close proximity of these deamidated residues to the catalytic site during E₂P confirmation. The deamidated residues may disrupt electrostatic interaction during E₁ phosphorylation, which may affect ion transport and signal transduction. Our findings suggest impaired regulation and compromised activity of ion channel proteins contribute to the pathophysiology of VaD.

KEYWORDS: dementia, Na⁺/K⁺-ATPase, ion channel proteins, iTRAQ, mass spectrometry



INTRODUCTION

In addition to Alzheimer's disease (AD), cerebrovascular disease is also a principal cause of age-related cognitive impairment.¹ AD and vascular dementia (VaD) are major contributors to disability, dependence, and mortality among older adults; by recent estimates, 36 million peoples are suffering with dementia worldwide with an addition of 4.6 million new cases annually.² Thus, further research is needed to understand the molecular events in the brain leading to dementia, and, in particular, the possible interlink between protein deamidation and dementia. With age, proteins undergo several spontaneous modifications that alter their structure and influence stability, folding, and biological function. Studies by Geiger and Clarke³ on aspartyl (Asp) and asparaginyl (Asn) deamidation, isomerization, and racemization revealed that L-Asp and L-Asn residues can be converted to four different isoforms (L-Asp, L-isoAsp, D-Asp, and D-isoAsp) via cyclic intermediates. Such transformations or isomerization denatures the protein, induces an

autoimmune response to self-proteins, and also leads to the accumulation of potential abnormal L-isoaspartyl residues that alters their 3-D structure, stability, folding, and, finally, loss of function.^{4–6} The accumulation of isomerized proteins has been linked to metabolic dysfunction in neuronal cells and neurodegenerative diseases.^{7,8} The occurrence or accumulation of such abnormal residues has been demonstrated in development and aging⁹ and has been shown to accelerate amyloid formation and alter amylin fiber structure, which may lead to AD.¹⁰

Isoaspartate (isoAsp) formation and its accumulation is a major source of protein damage. However, methyltransferases can recognize these changes and correct them through the

Special Issue: Proteomics of Human Diseases: Pathogenesis, Diagnosis, Prognosis, and Treatment

Received: February 13, 2014

Published: August 25, 2014

methyl esterification reaction. Thus, the enzyme protein L-isoaspartate (D-aspartate) O-methyltransferase (PIMT) functions as a protein repair enzyme and helps prevent the accumulation of dysfunctional proteins.¹¹ The proteomic analysis of PIMT knock-down mouse brain extract identified 22 proteins including proteins involved in regulating synaptic transmission (synapsins I and II, and dynamin-1) and cytoskeletal structure (e.g., alpha-, beta-tubulin) that were prone to isoAsp formation. The phosphorylation or acetylation of these proteins has been linked to the accumulation of isoAsp and protein damage. Furthermore, signal transduction remains a vital aspect in many diseases: the ion channel proteins or Na⁺/K⁺-ATPase are well-known for their role in ion transport across the plasma membrane. These ion channel proteins sustain Na⁺ and K⁺ gradient across the membrane, which is vital for maintaining the cellular electrical potential for neuronal signaling, muscle contraction, solute/substrate cotransportation, and so on. It also plays a major role in signal transduction, and several signaling pathways have been found to involve Na⁺/K⁺-ATPase.¹² However, to the best of our knowledge, ion channel protein regulation, their deamidation, and the role of PIMT have not been previously investigated in vascular causes of dementia.

Na⁺/K⁺-ATPase is a heterodimer of alpha- and beta-subunits. There are four and three different isoforms of alpha- and beta-subunits, respectively. The expression of both Na⁺/K⁺-ATPase alpha1- and alpha3-subunit in mammalian neurons is present, but its role is not known.^{13,14} A mutation in the gene coding Na⁺/K⁺-ATPase alpha3-subunit causes rapid onset of dystonia parkinsonism¹⁴ and familial hemiplegic migraine type-2, while its decline in activity is linked to impairment of learning and memory¹⁵ as Na⁺/K⁺-ATPase activity has been associated with the formation and persistence of long-term potential in neurons and glial cells through its involvement in the mechanisms of synaptic plasticity.^{16,17} However, deamidation of Na⁺/K⁺-ATPase ion channel proteins and the possible role of PIMT have not been previously examined. We hypothesize that the deamidation of ion-channel proteins interferes with the pumping of Na⁺ and K⁺ ions by Na⁺/K⁺-ATPase, affects signal transduction, and may be a cause of neurodegenerative diseases. Thus, the main aim of the current study was to profile the relative regulation of ion-channel proteins in VaD and age-matched controls and examine their deamidation so as to elucidate its role and possible association with PIMT.

MATERIALS AND METHODS

Patients and Clinical Assessments

This study analyzed brain tissues from age-matched non-demented controls and VaD patients. Frozen gray matter from the neocortex (Brodmann area, BA21) was acquired from the Newcastle Brain Tissue Resource (NBTR), Institute for Aging and Health, Newcastle University as part of the collection under Brains for Dementia Research, U.K. (<http://www.brainsfordementiaresearch.org.uk>). The details of the subjects are summarized in Table 1. The patients received current treatment either hypertension (a documented history of blood pressure greater than 140/90 mmHg), atrial fibrillation, ischemic heart disease, peripheral vascular disease, hypercholesterolemia, or diabetes (documented or treated). However, several of the aging controls also had vascular risk and were on current treatment for vascular factors (as previous described). Patients or controls were not treated for any other

Table 1. Characteristics of Subjects and Numbers of Samples for Control and VaD Patients

	control	VaD
number of patients	10	10
age of patients at death years (mean \pm SD) ^a	83.3 \pm 8.9	84.0 \pm 8.5
Braak staging		
0-II	5	9
III-IV	3	0
V-VI	0	0

^aSD: standard deviation.

neurological condition or depressive illness unless specified. VaD was diagnosed following guidelines by National Institute of Neurological Disorders and Stroke and Association Internationale pour la Recherché et l'Enseignement en Neurosciences (NINDS-AIREN).¹⁸ The pathological diagnosis of dementia was specified by the presence of lacunar infarcts or multiple microinfarcts, border-zone infarcts, microinfarcts (visible by microscopy), and small vessel disease in subcortical structures in the general absence of neurofibrillary tangles.¹⁹ None of the VaD cases satisfied diagnostic criteria for AD, as defined by Consortium to Establish a Registry for Alzheimer's Disease (CERAD).²⁰ The cognitive assessments were made using Mini-Mental State Examination (MMSE), which includes the 30-point scale to evaluate the cognitive functions that cover orientation, memory, and attention.²¹ The VaD patients had clinical dementia rating scores of 2 to 3.²² Informed consent was obtained from the guardians of the patients prior to donation of brain tissues, and approval for this study was granted by research ethics committees in the U.K. and in Singapore.

Experimental Design

The experimental design included 10 cases of VaD (age mean \pm SD; 84.00 \pm 8.50) and 10 age-matched control samples (age 80.30 \pm 8.9). Frozen gray matter from the neocortex (Brodmann area, BA21) previously dissected free of white matter and meninges were thawed on ice and centrifuged and proteins were acetone-precipitated. In brief, equal quantities of frozen tissues (w/w) were pooled in a group-wise manner and ground into fine powder using liquid nitrogen. The resultant fine power was suspended in a mixture of methanol (Merck, Darmstadt, Germany), chloroform, and water (J. T. Baker, Center Valley, PA) (1:1:2). The suspension was mixed and centrifuged at 15 000g for 5 min to obtain the pellet. The pellet was further washed using a mixture of methanol, chloroform, and water (4:1:3). The polar methanol–water phase was combined from consecutive steps, and proteins were precipitated by adding four volumes of previously chilled acetone. The protein pellet was washed with methanol and dissolved in 8 M urea with protease inhibitor cocktail (Complete (Roche; Mannheim, Germany)). Proteins from the control and test groups (200 μ g) were separated on SDS-PAGE, protein bands were visualized by staining with Coomassie Brilliant Blue, and each lane was sliced separately and cut into small pieces (~1 mm²). The gel slices were washed with 75% acetonitrile containing TEAB (25 mM). Following destaining, gel pieces were reduced with Tris 2-carboxyethyl phosphine hydrochloride (5 mM) and then alkylated with methylmethanethio-sulfonate (10 mM). Then, gel pieces were dehydrated using acetonitrile and subjected to protein digestion using sequencing-grade modified trypsin (Promega, Madison, WI) at 37 °C. The peptides were extracted using 50% acetonitrile and 5%

acetic acid and concentrated using concentrator (Eppendorf AG, Hamburg, Germany) for further iTRAQ reagent labeling. All experiments were performed in triplicate.

iTRAQ Labeling and LC–MS/MS Analysis

The iTRAQ labeling of dried peptides from control and test group was performed using 4-plex iTRAQ reagent Multiplex kit (Applied Biosystems, Foster City, CA) following manufacturer's protocol. The tryptic-digested peptides from pooled control and VaD ($n = 10$ for each group) were labeled by two iTRAQ tags (114: control, 115: VaD) of the 4-plex iTRAQ kit. The iTRAQ experiment was repeated thrice (experimental replicate = 3, named as Set1, Set2, and Set3) using the pooled digest. LC–MS/MS analysis was performed thrice (technical replicate = 3) for Set1 and Set2 and four times (technical replicate = 4) for Set3. We randomly selected 114 and 115 iTRAQ labels for this experiment. However, studies on their fragmentation behavior, accuracy, and precision of iTRAQ quantitation have been documented.^{23–26} Yet again, recently several researchers^{27–29} compared 4-plex, 8-plex- iTRAQ quantitative measurements of proteins and characterized bias, variability, fold changes, and fragmentation behaviors of different channels of 4-plex and 8-plex iTRAQ kits, which remain extremely important during selection of channels or tags. Mahoney et al.²⁹ demonstrated abundance distribution between technical replicates, between experiments, and between iTRAQ tags. In their study, postnormalization distributions demonstrated the removal of the global shifts in abundance and reduced variability in the data. They estimated the tag effect coefficient from the normalization model and found that the tag effect estimates did not reveal a consistent labeling bias and all were <0.125 on the log2 scale. As stated by Pichler et al.,²⁷ the isobaric labeling reagents (4-plex, 8-plex-iTRAQ, and 6-plex TMT) share common features like N-hydroxy-succinimide (NHS) chemistry, generation of reporter ions upon fragmentation, and balancer moiety, but they differ with regard to the number of channels available for multiplexing, mass shift induced by the modification, the atomic composition, and the number and types of heavy isotope atoms used. The labeling by three isobaric reagents (iTRAQ 4-plex, TMT 6-plex, and iTRAQ 8-plex) was compared with regards to the precision and dynamic range of quantification.²⁷ They observed approximately similar standard deviations for the log2 ratios of duplicate channels: 0.14 and 0.12 for duplicate channels 115:114 and 117:116, respectively, with iTRAQ 4-plex; 0.15 and 0.16 for 115:114 and 117:116 with iTRAQ 8-plex. These results suggest approximately similar precision for these isobaric labeling reagents on the level of peptide-spectrum matches. Pichler et al.²⁷ discovered higher identification yield using iTRAQ 4-plex compared with TMT 6-plex and iTRAQ 8-plex, while Pottiez et al.²⁸ observed more consistent ratios with 8-plex than 4-plex iTRAQ reagent without compromising protein identification. This study found 114:117 ratios lower than expected when 4-plex iTRAQ kit reagents were used. Our study used 114 and 115 tags from 4-plex iTRAQ kit and ratios 115:114 were reported. Karp et al.,²⁶ who used log ratios of 115:114, noted no significant intensity-dependent systematic bias and also observed consistent fragmentation efficiency across tags within an experiment.

iTRAQ labeled peptides were desalted using Sep-Pak C18 cartridges and then fractionated using HPLC. To reduce sample complexity and enhance separation, protein identification, and its confidence, we reconstituted the iTRAQ

labeled peptides in buffer A (10 mM ammonium acetate, 85% acetonitrile, 0.1% formic acid) and fractionated it by ERLIC method using a PolyWAX LP column (4.6 × 200 mm, 5 μ m, 300 Å) (PolyLC, Columbia, MD) adopting the HPLC system (Shimadzu) at a flow rate of 1.0 mL/min using our optimized laboratory protocol.^{30,31} The HPLC mobile phase consisted of buffer A (10 mM ammonium acetate, 85% acetonitrile, 0.1% acetic acid) and buffer B (30% acetonitrile, 0.1% formic acid), while 60 min gradient was 100% buffer A for 5 min, 0–36% buffer B for 25 min, 36–100% buffer B for 20 min, and 100% buffer B for 10 min at 1 mL/min flow rate. The HPLC chromatograms were recorded at 280 nm, and fractions were collected using automated fraction collector, concentrated using vacuum centrifuge, and reconstituted in 0.1% formic acid for LC–MS/MS analysis.

The LC–MS/MS analysis of HPLC-fractionated labeled samples was performed with a QStar Elite mass spectrometer (Applied Biosystems/MDS Sciex) coupled to online microflow MDLC system. The iTRAQ labeled peptides were separated on a home-packed nanobored C18 column with a picofrit nanospray tip (75 μ m ID × 15 cm, 5 μ m particles). Each iTRAQ-labeled peptides fraction of set 1 was sequentially injected in triplicate. Similarly, set 2 was analyzed in triplicate, while set 3 was analyzed by the LC–MS/MS using 60 min gradient for four times. The QSTAR Elite was set to positive ion mode using Analyst QS 2.0 software (Applied Biosystems) for data acquisition. The precursors with a mass range of 300–1600 m/z and calculated charge from +2 to +5 were selected for fragmentation. Peptides above five-count threshold were selected for MS/MS, and each selected target ion was dynamically excluded for 20s with a mass tolerance of 0.1 Da. Smart information-dependent acquisition was activated with automatic collision energy and automatic MS/MS accumulation. The fragment intensity multiplier was set to 20, and maximum accumulation time was 2 s.

Mass Spectrometric Data Search and Analysis

A total of ten sets of data acquired from the technical and experimental replicates was further processed using ProteinPilot software. The peak list generation, protein identification, and peptide quantification were performed using ProteinPilot software 3.0 (revision number 114732; Applied Biosystems, Foster City, CA). The concatenated target-decoy UniProt human database (sequence 87 187, downloaded on 12 March 2012) was used for data search. The database search for Set1, Set2, and Set3 (biological replicates as defined above) and their technical replicates were performed separately, and the mean values with standard deviations of the proteins that were quantified in at least two sets were reported in this study. The peptide identification was performed with Paragon algorithm (3.0.0.0, 113442) in ProteinPilot software and further processed with Pro Group algorithm where isoform-specific quantification was implemented to trace the differences between expressions of various isoforms. User-defined parameters in ProteinPilot software were: (i) sample type: iTRAQ 4-plex (peptide-labeled); (ii) cysteine alkylation: methylmethanethiosulfonate; (iii) digestion: trypsin; (iv) instrument: QSTAR Elite ESI; (v) special factors: urea denaturation; (vi) species: none; (vii) specify processing: quantitate, bias and background correction; (viii) identification focus: biological modifications and amino acid substitutions using DB, a concatenated target, and decoy Uniport human database database; and (ix) search effort: thorough. The default precursor and

MS/MS tolerance for QSTAR ESI-MS instrument were adopted automatically by the software. The false discovery rates (FDRs) of both peptide and protein identification were set to be <1% (FDR = 2.0*decoy hits/total hits). The peptide for protein quantification was automatically selected by Pro Group algorithm to calculate the iTRAQ ratio, *p* value, and other parameters using the following criteria: (a) the peptide was suitable for quantitation (iTRAQ reporter area >0); (b) the peptide was identified with good confidence; and (c) the peptide was not shared with another protein that had been identified with higher confidence. On top of these criteria, that is, Pro Group quantified proteins, we selected only proteins that were iTRAQ-quantified with more than two unique peptides with >95% confidence in at least two biological replicates and two technical replicates. We applied iTRAQ cut off values of ≤ 0.80 for down-regulation and ≥ 1.2 for up-regulation.

RESULTS AND DISCUSSION

VaD is the second most common cause of age-related dementia after AD, and acquaintance of its pathophysiology is lagging behind due to limited knowledge of the molecular events driving vascular and parenchymal changes in the brain. As agreed with the complexity and heterogeneity of cerebrovascular disorder and the occurrence of comorbidities in VaD patients, it is most likely that multiple protein candidates rather than a small number of protein present in network are perturbed. Protein quantification through the incorporation of stable isotopes has become a central technique in modern proteomics research that made it possible to explore global relative quantitation of proteins across various biological samples in a single experiment. Taking an advantage of this technique and to elucidate the perturbed pathways contributing to pathophysiology of VaD, iTRAQ-based quantitative proteomics was applied on brain samples to profile relative protein expression in pathologically confirmed cases of VaD and matched non-neurological controls. Again, it has been put forward that through deamidation, Asn and Gln may serve as molecular clocks that time biological processes including protein turnover, homeostatic control, and organism development, aging and many more.^{32–35} Protein deamidation causes structural changes and functional inactivation and also enhancement in the protein aggregation process, which is considered to be one of the progression factors in AD. Therefore, this study further targeted PTM of regulated sodium potassium transporting ATPase and located deamidation site by adopting the 3D structure of Na⁺/K⁺-ATPase.

Estimation of Threshold and Bioinformatics Analysis

A strict cutoff of unused protein score ≥ 2 (which corresponds to a confidence limit of 99%) as the qualification criteria and FDR of <1.0% was employed to minimize the false-positive identification of proteins. To obtain quality and high confident data, ten replicates (including biological and technical replicates) were analyzed, and the average data with standard deviation were reported in this study. The proteins identified with at least two peptides in each run were further considered. Using these criteria, we iTRAQ-quantified 1315 ± 240 proteins (Table S1, Supporting Information). To these proteins, we applied iTRAQ cut-off values of ≤ 0.80 for down-regulation and ≥ 1.2 for up-regulation. Although this study iTRAQ-quantified 1315 ± 240 proteins, here we limit our objective to ion-channel

proteins. These proteins were subjected to the next stage of bioinformatics to identify motif and deamidation sites.

iTRAQ Quantification and Regulation of Ion-Channel Proteins

To combat the dissipation of the concentration and electrical gradients of ions, Na⁺/K⁺-ATPase play critical role in regulating concentration of Na⁺, K⁺ inside and outside the cell. However, there is limited data on the role(s) of ion-channel proteins such as the voltage-dependent anion-selective channel protein 1 (VDAC1), which participate in the formation of the permeability transition pore complex (PTPC). In our study, when brain tissue samples from VaD subjects were analyzed using the iTRAQ quantitative technique, 50% of the ion-channel proteins identified including voltage-dependent anion-selective channel protein 1 (VDAC1) and voltage-dependent anion-selective channel protein 2 (VDAC2) of VaD subjects were down-regulated when compared with age-matched controls (Figure 1). Because a high level of VDAC1 expression

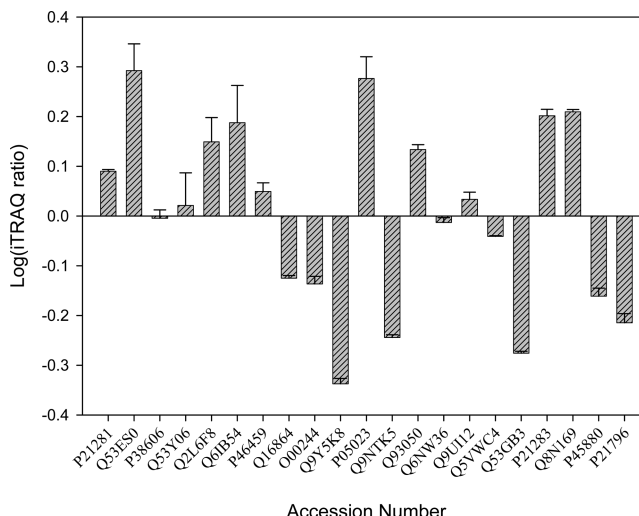


Figure 1. Relative expression of ion-channel proteins in dementia subjects (P21281: V-type proton ATPase subunit B, brain isoform; Q53ES0: Na⁺/K⁺-ATPase alpha 3 subunit variant; P38606: V-type proton ATPase catalytic subunit A; Q53Y06: ATPase, H⁺ transporting; Q2L6F8: ATPase, H⁺ transporting; Q6IB54: ATP synthase, H⁺ transporting; P46459: vesicle-fusing ATPase; Q16864: V-type proton ATPase subunit F; O00244: Copper transport protein; Q9Y5K8: V-type proton ATPase subunit D; P05023: sodium/potassium-transporting ATPase subunit alpha-1; Q9NTK5: Obg-like ATPase 1; Q93050: V-type proton ATPase 116 kDa subunit 1 isoform 1; Q6NW36: proteasome 26S subunit, ATPase, 1; Q9UI12: V-type proton ATPase subunit H; Q5VWC4: proteasome 26S subunit, non-ATPase, 4; Q53GB3: ATP synthase, H⁺ transporting; P21283: V-type proton ATPase subunit C 1; Q8N169: solute carrier family 1, glutamate transporter; P45880: voltage-dependent anion-selective channel protein 2; P21796: voltage-dependent anion-selective channel protein 1).

has been reported in brain,³⁶ the down-regulation of these VDAC proteins can lead to reduced mitochondrial function enhancing oxidative stress impairing neural function in VaD patients. Proteins like V-type proton ATPase subunit D (VATD), ATP synthase, H⁺ transporting, mitochondrial F0 complex, subunit b isoform (ATP5F1), Obg-like ATPase 1 (OLA1), and V-type proton ATPase subunit F (VATF) (Table 2) were also down-regulated in VaD patients. Down-regulation of protein like VATD, ATP5F1, OLA1, and VATF involved in energy production results into reduced energy production, cell

Table 2. iTRAQ-Quantified PIMT and Ion-Channel Proteins Regulated in Demented Patients^a

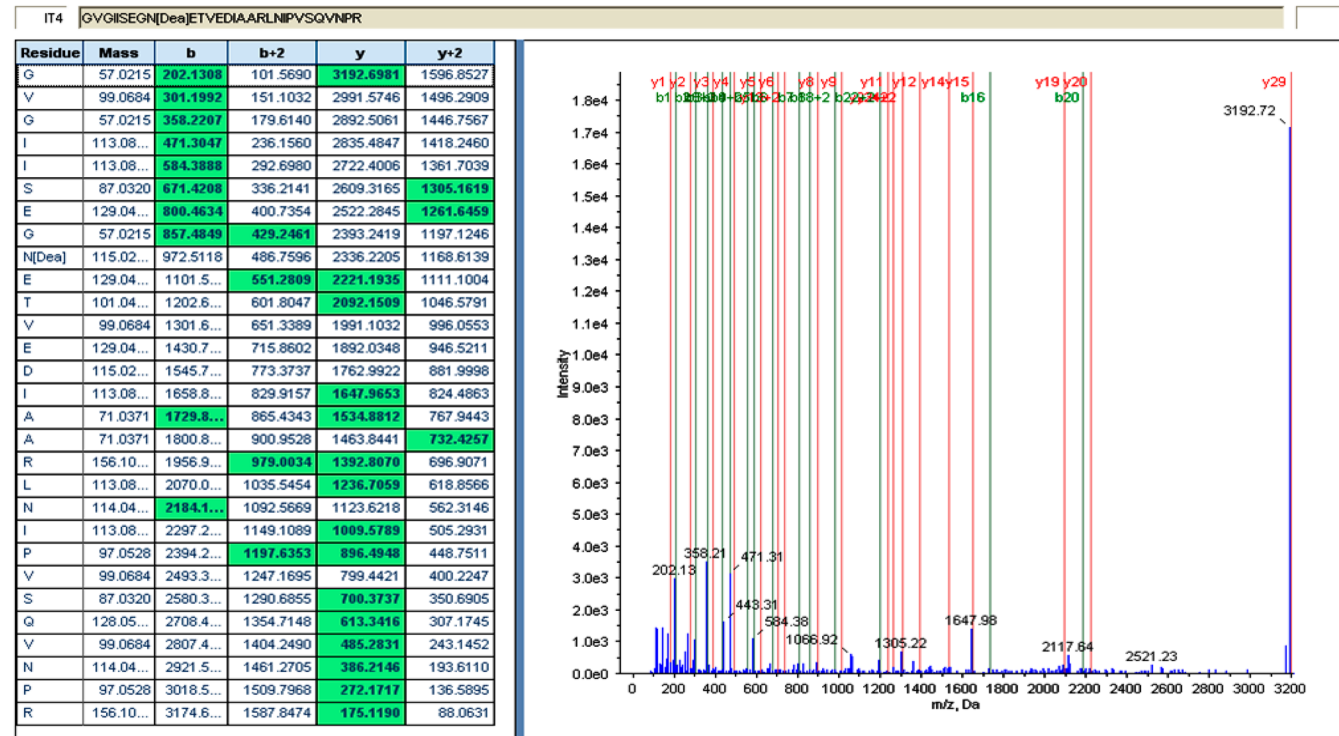
protein score	total protein score	% coverage	accession	protein	peptides (95%)	115;114
22.21 ± 9.4	23.5 ± 7.5	87.2 ± 9.6	P22061	protein-1-isoaspartate (D-aspartate) O-methyltransferase	19 ± 8	1.31 ± 0.26
59.4 ± 20.2	59.4 ± 20.2	66.2 ± 9.6	P55072	transitional endoplasmic reticulum ATPase	34 ± 14	0.64 ± 0.05
48.2 ± 9.8	48.2 ± 9.8	76.9 ± 6.0	P21281	V-type proton ATPase subunit B, brain isoform	32 ± 11	1.23 ± 0.18
24.6 ± 6.0	27.7 ± 10.1	36.2 ± 7.9	Q53ES0	Na ⁺ /K ⁺ -ATPase alpha 3 subunit variant (fragment)	14 ± 6	1.96 ± 0.46
28.2 ± 7.6	28.2 ± 7.6	54.3 ± 11.8	P38606	V-type proton ATPase catalytic subunit A	18 ± 7	0.99 ± 0.13
29.1 ± 6.0	29.1 ± 6.0	74.8 ± 13.8	Q53Y06	ATPase, H ⁺ transporting, lysosomal 31 kDa, V1 subunit E isoform 1	21 ± 7	1.05 ± 0.14
22.7 ± 4.0	22.7 ± 4.0	88.3 ± 6.7	Q2L6F8	ATPase, H ⁺ transporting, lysosomal 13 kDa, V1 subunit G2	30 ± 12	1.41 ± 0.18
24.8 ± 8.4	24.8 ± 8.4	86.1 ± 10.1	Q6IB54	ATP synthase, H ⁺ transporting, mitochondrial F0 complex, subunit F6, isoform CRA	17 ± 6	1.54 ± 0.18
18.5 ± 6.1	20.8 ± 6.8	44.5 ± 12.4	P46459	vesicle-fusing ATPase	10 ± 4	1.12 ± 0.14
5.7 ± 2.2	7.0 ± 4.6	53.4 ± 24.7	Q16864	V-type proton ATPase subunit F	5 ± 3	0.75 ± 0.07
8.1 ± 1.6	7.8 ± 1.7	71.3 ± 15.4	O00244	copper transport protein ATOX1	4 ± 1	0.73 ± 0.13
5.6 ± 2.9	3.9 ± 3.6	30.0 ± 20.0	Q9Y5K8	V-type proton ATPase subunit D	2 ± 2	0.46 ± 0.09
6.1 ± 1.1	18.8 ± 4.3	32.6 ± 7.9	P05023	sodium/potassium-transporting ATPase subunit alpha-1	10 ± 3	1.89 ± 1.13
7.4 ± 1.5	7.4 ± 1.5	48.0 ± 13.0	P61970	nuclear transport factor 2	5 ± 2	0.97 ± 0.10
5.6 ± 2.4	5.0 ± 3.0	27.0 ± 12.8	Q9NTK5	Obg-like ATPase 1	2 ± 2	0.57 ± 0.05
3.1 ± 1.2	3.5 ± 1.4	12.1 ± 5.5	Q93050	V-type proton ATPase 116 kDa subunit a isoform 1	2 ± 1	1.36 ± 0.16
5.5 ± 2.0	5.1 ± 2.6	24.5 ± 7.5	Q6NW36	proteasome (prosome, macropain) 26S subunit, ATPase, 1	2 ± 1	0.97 ± 0.11
4.7 ± 0.0	2.6 ± 2.0	13.2 ± 8.0	A8KL43	cDNA FLJ7534;2, highly similar to <i>Homosapiens</i> solute carrier family 12, (potassium-chloride transporter) member 5 (SLC12A5), mRNA	2 ± 1	0.02, ± 0.01
3.1 ± 1.1	3.1 ± 1.1	20.8 ± 8.6	Q9U112	V-type proton ATPase subunit H	2 ± 1	1.08 ± 0.12
4.3 ± 1.2	4.3 ± 1.1	24.4 ± 6.5	Q5VW4	proteasome (prosome, macropain) 26S subunit, non-ATPase, 4	2 ± 1	0.91 ± 0.07
6.0 ± 4.0	4.6 ± 4.5	30.7 ± 20.1	Q53GB3	ATP synthase, H ⁺ transporting, mitochondrial F0 complex, subunit b isoform 1 variant (fragment)	2 ± 2	0.53 ± 0.07
16.7 ± 3.9	18.2 ± 4.1	49.0 ± 6.7	P45880	voltage-dependent anion-selective channel protein 2	12 ± 3	0.69 ± 0.07
45.2 ± 7.4	45.2 ± 7.4	86.0 ± 6.8	P21796	voltage-dependent anion-selective channel protein 1	32 ± 8	0.61 ± 0.04

^aTransport proteins iTRAQ-quantified with unused score ≥2 and with ≥2 peptides are listed.

Table 3. iTRAQ-Quantified Deamidated Ion-Channel Proteins with Their Peptide Sequence and Deamidation Site

accessions	GeneSym	name of protein	peptide
P05023	ATP1A1	sodium/potassium-transporting ATPase subunit alpha-1	VDNSSLTGESEPQ#TRS
P50993	ATP1A2	sodium/potassium-transporting ATPase subunit alpha-2	GVGIISEGN#ETVEDIAARL
Q53ES0; P13637	ATP1A3	sodium/potassium-transporting ATPase subunit alpha-3	GVGIISEGN#ETVEDIAARLNIPVSQVNPR
P50993	ATP1A2	sodium/potassium-transporting ATPase subunit alpha-2	LIFDN#LK
P50993	ATP1A2	sodium/potassium-transporting ATPase subunit alpha-2	LN#IPMSQVNPR
P05026	ATP1B1	sodium/potassium-transporting ATPase subunit beta-1	VAPPGLTQ#IPQIQQK

Fragmentation Evidence for Peptide

Figure 2. MS/MS spectrum of sodium/potassium transporting ATPase subunit alpha 3 deamidated peptide that show deamidation site at N*. The spectrum shows the peptide fragmentation pattern and is labeled with both *b* and *y* ions.

exhaustion, and enhanced cell death.³⁷ Proteins like sodium/potassium-transporting ATPase subunit alpha-1 (ATP1A1) and Na⁺/K⁺-ATPase alpha 3 subunit variant (ATP1A3), which catalyze the hydrolysis of ATP coupled to the exchange of Na⁺ and K⁺ ions, were up-regulated in VaD patients. The current findings suggest that Na⁺/K⁺-ATPase could be an important target for dementia, particularly VaD.

We noted up-regulation of glutamate transporter (solute carrier family 1-SLC1). Woltjer et al.³⁸ also found significant increase in levels of glutamate transporters and excitatory amino-acid transporters (EAAT2) in patients with AD, while their level in clinical dementia rating subjects was intermediate elevated. The results by Kirvell et al.³⁹ on the homogenates prepared from gray matter from two neocortical regions (Brodmann area BA 9 and BA 20) showed lower expression of EAAT2, but its concentration could not correlate with either CAMCOG (Cambridge Assessment of Mental Health for the Elderly, Section B) total score or CAMCOG memory score. Again, EAATs transporting L-glutamate and L-aspartate are mostly expressed in glial cells (EAAT1 and EAAT2) and neurons (EAAT3 and EAAT4), where they specifically regulate extracellular glutamate levels at both synaptic and extrasynaptic sites.⁴⁰ It is well-established that

EAATs play critical roles in the maintenance of normal excitatory synaptic transmission, protection of neurons from the excitotoxic action of excessive glutamate, and regulation of glutamate-mediated neuroplasticity.⁴⁰ Dysfunction of EAATs has been implicated in a variety of neurodegenerative diseases such as amyotrophic lateral sclerosis, Parkinson's disease, AD, Huntington's disease, and glaucoma and other neurological diseases including ischemia, epilepsy, ataxia, and HIV-associated dementia.^{40–42} Again, these glutamate transporters are sodium-dependent proteins that rely on ion gradients generated by Na⁺/K⁺-ATPase.¹² In addition, ATP1A1 and ATP1A3 and proteins such as V-type proton ATPase subunit B, V-type proton ATPase subunit C1, and V-type proton ATPase 116 kDa subunit A isoform 1 were also up-regulated in VaD patients, as were ATPase, H⁺ transporting, subunit G2 and ATP synthase, H⁺ transporting, subunit F6 that regulates electrogenic proton pump by acidifying intracellular compartments of cells. The limitation of this study is the small amount of the starting tissues that did not allow validation of the candidate proteins as the availability of post-mortem brain tissue of VaD is relatively limited compared with AD.

Deamidation of Ion-Channel Proteins

In addition to biological metabolic pathway regulation, protein post-translational modifications such as deamidation are

Fragmentation Evidence for Peptide

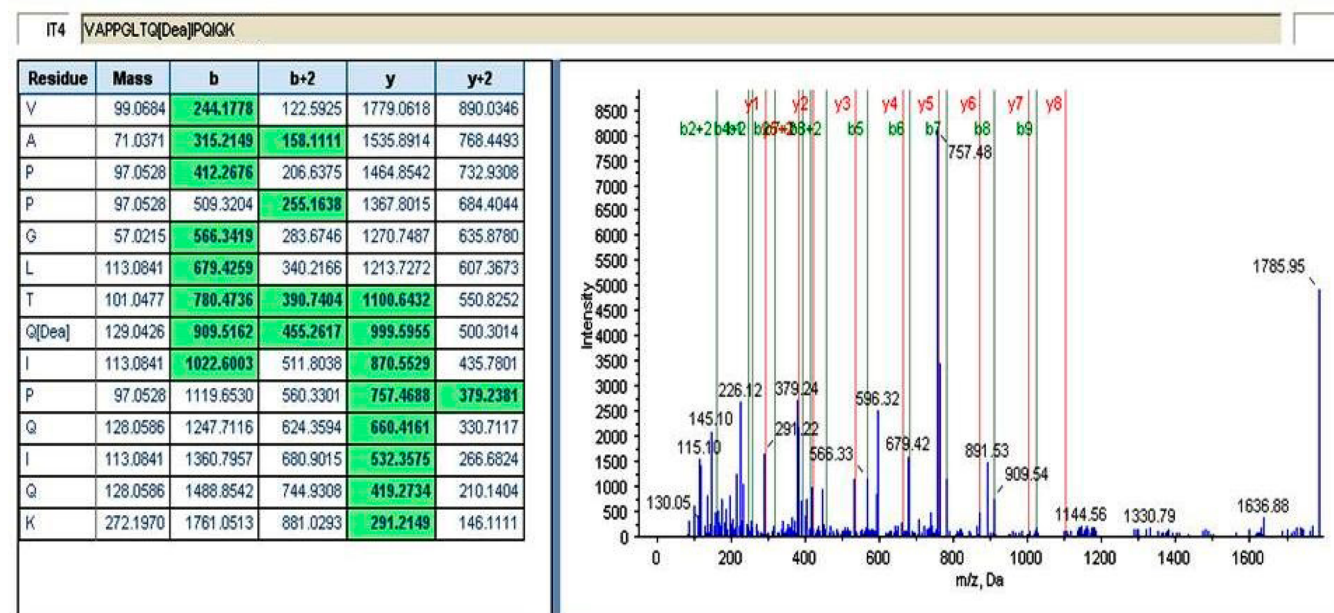


Figure 3. MS/MS spectra of sodium/potassium transporting ATPase subunit beta 1 peptide that show deamidation site at Q*. The spectrum shows the peptide fragmentation pattern and is labeled with both *b* and *y* ions.

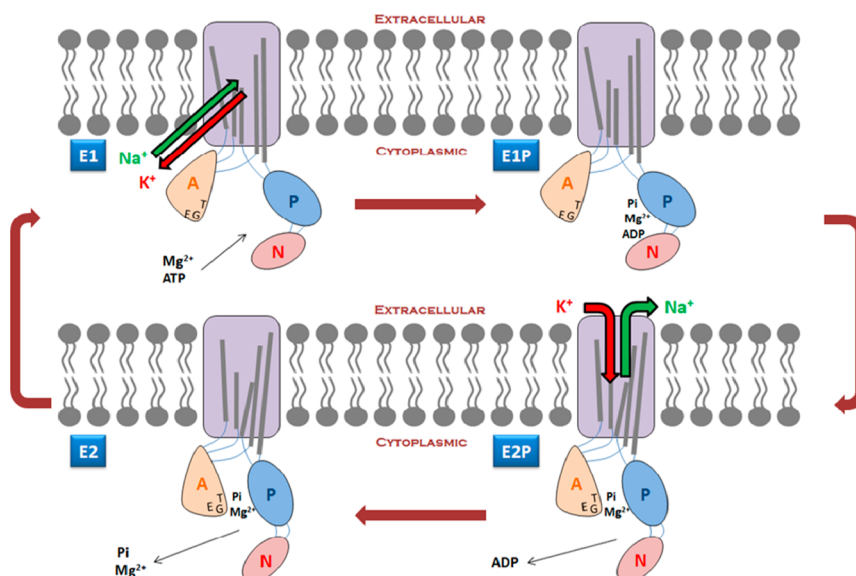


Figure 4. Simplified schematic of sodium/potassium ion transport in Na^+/K^+ -ATPase. The α -subunit consists of four domains: N (nucleotide-binding), A (actuator), P (phosphorylation), and M (membrane) domains. The major conformational changes during E_1P to E_2P transition is the 35° rotation of P domain, the rotation of N-domain away from the P-domain, and the rotation and translation of A domain that relocate the TGE sequence near to the catalytic site.^{67–69}

important^{33,34,43–47} but often ignored. Identified ion-channel protein peptides with deamidation sites are listed in Table 3. ATP1A1 and ATP1A2 showed deamidation (Figures 2 and 3, Figures S1–S7 Supporting Information). No published data exist on the deamidation of ATP1A1, ATP1A2, and ATP1A3, however, it has been documented that the deamidation of channel forming prion protein alters channel activity and causes progressive neurodegeneration.⁴⁸ Exposure of channel forming PrP(106–126) peptide to low concentration of Cu^{2+} causes change in conformation of this peptide, leading to changes in current transition. Thus, deamidation of channel forming

peptide induces abnormal changes in signal transduction and causes neurodegenerative disease. Interestingly, the quantitative deamidation by integrating chromatograms showing N-deamidation and Q-deamidation revealed 1.63 and 1.46 ratios (115/114), indicating significantly higher deamidation in VaD patients. Again, our data set showed expression of Cu^{2+} transport protein and deamidated ATP1A1 and ATP1A2. According to Robinson,⁴³ protein deamidation introduces a negative charge at the deamidation site and sometimes also leads to beta-isomerization. Thus, deamidation of ATP1A1 and ATP1A2 alters total charge of this protein subunit, leading to

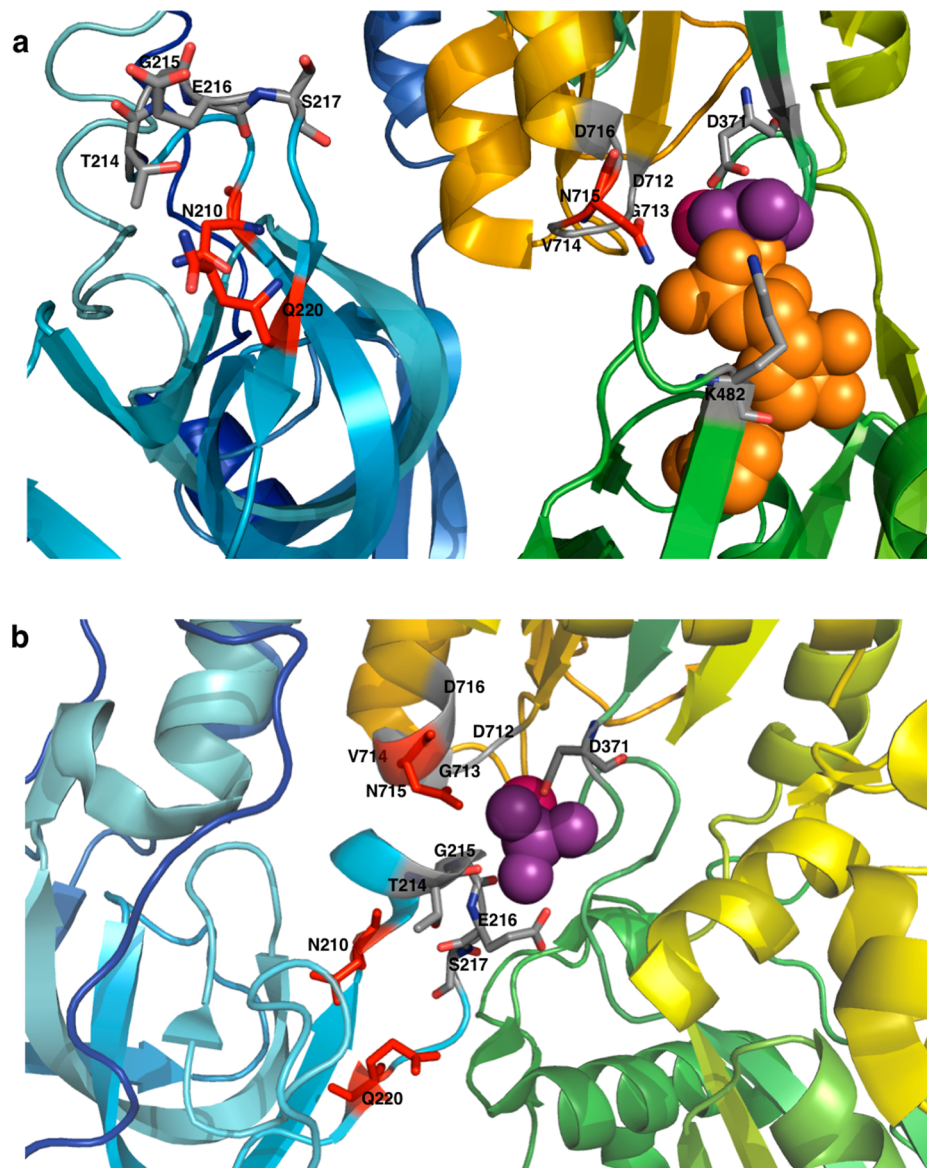


Figure 5. Structural models of Na^+/K^+ -ATPase catalytic site in (a) E_1P^{68} and (b) E_2P^{67} conformations (PDB ID 4HQJ and 2ZXE, respectively). In both a and b, color changes gradually amino-terminal (blue) to carboxyl-terminal (red): A domain is in blue and cyan, P domain is in yellow, and N domain is in green. Notable deamidated residues, N210, D220, and N715, are in red, whereas highly conserved sequences, $^{214}\text{TGES}$, $^{712}\text{DGVND}$, Asp 371 , and Lys 482 , are in gray. Magnesium ion is in magenta, ADP is in orange, and phosphate analogue is in purple. In E_2P state (b), $^{712}\text{TGES}$ is located in close proximity to the catalytic site compared with E_1P state (a). Structural models is visualized and prepared in The PyMOL Molecular Graphics System, version 1.3 Schrödinger.

conformational change at the Mg^{2+} , Cu^{2+} binding site. This further affects the conductance of ions, resting membrane potential, action potential, and signal transduction. However, further detailed study is required.

Na⁺/K⁺-ATPase Deamidated Sites in Structural Models

Na^+/K^+ -ATPase is a heterodimer of α -, β -, and tissue-specific regulatory γ -subunit. The α -subunit consists of four domains that rearrange to change the conformations of the Na^+/K^+ -ATPase while translocating ions via ATP hydrolysis. The reactions linking ion transport to ATP hydrolysis through conformational changes are shown in Figure 4. Three of the identified deamidated residues in ATP1A1 and ATP1A2 were located in close proximity to highly conserved sequences, which is important for Na^+/K^+ -ATPase activity. Mutation of Asn 715 to Ala reduced Na^+/K^+ -ATPase affinity for Mg^{2+} by four-fold in

the E_1 conformation, which further affected dephosphorylation of Na^+/K^+ -ATPase and its activity.⁴⁹ Thus, Asn 715 play a major role in maintaining activity of Na^+/K^+ -ATPase. As can be seen from Figure 5, Asn 210 and Gln 220 are located near a conserved $^{214}\text{TGES}$ sequence in the domain A, whereas Asn 715 is in the conserved $^{712}\text{DGVND}$ sequence. Restated, structural models of Na^+/K^+ -ATPase in E_1P and E_2P conformations placed these three deamidated residues in close proximity to the catalytic site during the E_2P conformation. In fact, the conserved $^{214}\text{TGES}$ of domain A, which is isolated in the E_1P form, makes contact with the phosphorylation site and becomes catalytically important in the E_2P conformation.⁵⁰ During the E_1P to E_2P transition, $^{214}\text{TGES}$ in domain A rotates close to the catalytic site and docks onto the P domain.⁵¹ As reported by Toustrup-Jensen et al.,⁵⁰ $^{214}\text{TGES}$ is important in E_2P dephosphorylation that plays a major role in facilitating and positioning an

attacking water molecule in a nucleophilic attack of the phosphorylated Asp³⁷¹ or by interacting with phosphate group. According to Patchornik,⁵¹ ²¹⁴TGES sequence coordinates Mg²⁺ in E₂P and E₂ states, while, as confirmed by Goldshleger et al.,⁵² conformational transition from E₁P to E₂P is associated with a change in Mg²⁺ ligation where glutamic acid residue of ²¹⁴TGES is involved in Mg²⁺ coordination in E₂P. Thus, deamidation of Asn²¹⁰ and Gln²²⁰ flanking the ²¹⁴TGES on both sides interferes with ²¹⁴TGES repositioning near the catalytic site in E₂P, interrupting any interactions that ²¹⁴TGES formed near the catalytic site. Thus, deamidation of residues like Asn²¹⁰ and Gln²²⁰ causes defects in phosphorylation and dephosphorylation mechanism, further affecting ATP hydrolysis and energy supply for ATP-coupled ion transport. In nerve cells, Na⁺/K⁺-ATPase generates gradient of both sodium and potassium ions and propagates electrical signals that travel along nerves. However, this electrical signal-transfer process requires ATP to generate resting potentials, and defects in it prevent proper functioning of the nervous system.

According to Faller,⁵³ Mg²⁺ counterbalances the negative charge formed in the transition state and in the leaving carboxyl group during phosphorylation.⁵³ Again, as depicted by Robinson,⁴³ protein deamidation introduces a negative charge at the deamidation site. Interestingly, our study noted the deamidation of three residues located in close proximity to catalytic site, which disrupts electrostatic interactions during E₁ phosphorylation to E₁P. Na⁺/K⁺-ATPase plays critical role in maintaining ionic gradients for neuronal signaling, and any defects in them affect the signaling mechanism, leading to multiple neurological disorders, AD, learning, and memory.^{54–57} Thus, our study reports impaired regulation of Na⁺/K⁺-ATPase and its compromised activity as a major cause of pathogenesis of VaD.

Quantitative Expression of Protein L-Isoaspartate (D-Aspartate) O-Methyltransferase

Asparaginyl and aspartyl residues are the most labile amino acids of the protein that undergo modification, yielding both isoaspartyl (isomerization) and normal aspartyl residues.⁵⁴ Proteins containing L-isoaspartyl and D-aspartyl residues have distorted structures and biological activity. However, PIMT can recognize these abnormal residues and convert them to the normal L-aspartyl form.^{55,56} Kosugi et al.⁵⁷ established PIMT-knockdown cells using a short interfering RNA expression system and exemplified abnormalities in intracellular signaling pathways, leading to significant accumulation of proteins with racemized D-aspartyl residues in PIMT-knockdown cells. The knockout or transgenic mice model showing epileptic phenotype has deduced molecular mechanism including ion-channel genes and genes regulating the synaptic release of neurotransmitters for epileptogenesis.^{58,59} Thus, several researchers concluded that PIMT repair of abnormal protein is necessary to maintain normal signaling.^{55,57,60}

In this study, PIMT was identified with unused score of 22.2 and percentage coverage 87.2. We found upregulation of PIMT in brain tissue of dementia subjects when compared with age-matched control. The down-regulation of VDAC proteins may enhance oxidative stress, stimulating overexpression of PIMT. The PIMT activity has been detected in all vertebrates, but significantly high level of activities and repair has been reported in brain tissue.⁶⁰ In our PTM study, we noted deamidated PIMT. Although up-regulation of ion-channel proteins and further loss of their function due to deamidation could be

compensated by overexpression of PIMT, the effects of deamidated PIMT has not yet been explored. Thus, we propose the deamidation of PIMT could influence its potential to recognize abnormal residues or affect its capability to convert isoaspartyl to the normal L-aspartyl form.

Methyltransferase specifically recognizes abnormal D-aspartyl and L-isoaspartyl residues, methyl-esterifies them, and rapidly converts to succinimidyl residues in a nonenzymatic reaction, followed by spontaneous hydrolysis to native L-aspartyl residues.⁶⁰ This prevents further accumulation of abnormal proteins and also restores protein configuration and function by eliminating L-isoaspartyl linkages and racemized D-aspartyl residues.^{56,61,62} However, deamidation of PIMT might be causing defects in its protein repairing function and leads to significantly high accumulation of abnormal isoaspartyl and contributes to neuronal degeneration. The deamidation of ion-channel proteins introduces defects in the phosphorylation and dephosphorylation mechanism and ATP-coupled translocation of Na⁺, K⁺ by Na⁺/K⁺-ATPase. Modulation of Na⁺/K⁺-ATPase activity affects neurotransmitter signaling and neural activity, while inhibition by ouabain decreases norepinephrine,⁶³ dopamine, and serotonin reuptake⁶⁴ and increases acetylcholine release.⁶⁵ Inhibition of Na⁺/K⁺-ATPase also impairs spatial and other forms of learning.⁶⁶

CONCLUSIONS

Dementia is caused by brain damage leading to impaired cognition, behavior, and psychiatric symptoms. Na⁺/K⁺-ATPase not only transports ions but also is involved in many signaling events that are regulated by protein–protein interactions involving Na⁺/K⁺-ATPase. iTRAQ quantitative profile revealed significant dysregulation of sodium–potassium transporting Na⁺/K⁺-ATPase with up-regulation of PIMT. This study noted deamidation of ATP1A1 and ATP1A2 subunits of Na⁺/K⁺-ATPase and abnormal isoaspartyl repairing PIMT. The overall data analysis revealed up-regulation of sodium–potassium transporting Na⁺/K⁺-ATPase, down-regulation of voltage-dependent anion-selective channel proteins, deamidation in catalytic subunits of sodium–potassium transporting ATPase, and defective PIMT, which could affect membrane polarization and signal transfer and hence be a cause of and treatment target in VaD.

ASSOCIATED CONTENT

Supporting Information

Table S1. iTRAQ-quantified proteins. Figure S1. MS/MS spectrum of GVGISEGN*ETVEDIAARLNIPVSQVNPR (potassium transporting ATPase subunit alpha2) showing fragmentation evidence and modification assigned by ProteinPilot. Figure S2. MS/MS spectrum of VAPPGLTQIPQIQ*K (sodium/potassium transporting ATPase subunit beta1) showing fragmentation evidence and modification assigned by ProteinPilot. Figure S3. MS/MS spectrum of LN*IPMSQVNPR (sodium/potassium transporting ATPase subunit alpha 2) showing fragmentation evidence and modification assigned by ProteinPilot. Figure S4. MS/MS spectrum of GVGIISEGN#ETVEDIAARG (sodium/potassium transporting ATPase subunit alpha 2) showing fragmentation evidence and modification assigned by ProteinPilot. Figure S5. MS/MS spectrum of VAPPGLTQ#IPQIQQ (sodium/potassium-transferring ATPase subunit beta-1) showing fragmentation evidence and modification assigned by ProteinPilot. Figure S6. MS/MS spectrum of

LN#IP (sodium/potassium-transporting ATPase subunit alpha 2) showing fragmentation evidence and modification assigned by ProteinPilot. Figure S7. MS/MS spectrum of VDN#SSLTGE-SEPQTR (sodium/potassium-transporting ATPase subunit alpha-1) showing fragmentation evidence and modification assigned by ProteinPilot. This material is available free of charge via the Internet at <http://pubs.acs.org>.

AUTHOR INFORMATION

Corresponding Author

*Tel: +65:6514-1006. Fax: +65:6791-3856. E-mail: sksze@ntu.edu.sg.

Notes

The authors declare no competing financial interest.

ACKNOWLEDGMENTS

We thank the patients, families, and clinical staff for their cooperation during this investigation study. Tissue for this study was collected by the NBTR, which is funded in part by a grant from the U.K. Medical Research Council (MRC; G0400074), by the Newcastle NIHR Biomedical Research Centre in Ageing and Age Related Diseases award to the Newcastle upon Tyne Hospitals NHS Foundation Trust, and by a grant from the Alzheimer's Society and Alzheimer's Research U.K. (ARUK) as part of the Brains for Dementia Research Project. We thank Dr. Arnab Datta for helpful experimental discussion/assistance. This research work was supported by the Singapore National Research Foundation under its CBRG grant (NMRC/CBRG/0004/2012) and administered by the Singapore Ministry of Health's National Medical Research Council and CSA grant (NMRC/CSA/032/2011). R.N.K. is supported by grants from the Newcastle Centre for Brain Ageing and Vitality, U.K. MRC (G0500247), and the Alzheimer's Research U.K.

REFERENCES

- (1) Kalaria, R. N. Cerebrovascular disease and mechanisms of cognitive impairment: evidence from clinicopathological studies in humans. *Stroke* **2012**, *43* (9), 2526–2534.
- (2) Llibre, J. J. Aging and Dementia: Implications for Cuba's Research Community, Public Health and Society. *MEDICC Rev.* **2013**, *15* (4), 54–59.
- (3) Geiger, T.; Clarke, S. Deamidation, isomerization, and racemization at asparaginyl and aspartyl residues in peptides. Succinimide-linked reactions that contribute to protein degradation. *J. Biol. Chem.* **1987**, *262* (2), 785–794.
- (4) Mamula, M. J.; Gee, R. J.; Elliott, J. I.; Sette, A.; Southwood, S.; Jones, P. J.; Blier, P. R. Isoaspartyl post-translational modification triggers autoimmune responses to self-proteins. *J. Biol. Chem.* **1999**, *274* (32), 22321–22327.
- (5) Anderton, S. M. Post-translational modifications of self antigens: implications for autoimmunity. *Curr. Opin. Immunol.* **2004**, *16* (6), 753–758.
- (6) Doyle, H. A.; Mamula, M. J. Post-translational protein modifications in antigen recognition and autoimmunity. *Trends Immunol.* **2001**, *22* (8), 443–449.
- (7) Desrosiers, R. R.; Fanelus, I. Damaged proteins bearing L-isoaspartyl residues and aging: a dynamic equilibrium between generation of isomerized forms and repair by PIMT. *Curr. Aging Sci.* **2011**, *4* (1), 8–18.
- (8) Clarke, S. Aging as war between chemical and biochemical processes: protein methylation and the recognition of age-damaged proteins for repair. *Ageing Res. Rev.* **2003**, *2* (3), 263–285.
- (9) Hasan, Q.; Alluri, R. V.; Rao, P.; Ahuja, Y. R. Role of glutamine deamidation in neurodegenerative diseases associated with triplet repeat expansions: a hypothesis. *J. Mol. Neurosci.* **2006**, *29* (1), 29–33.
- (10) Dunkelberger, E. B.; Buchanan, L. E.; Marek, P.; Cao, P.; Raleigh, D. P.; Zanni, M. T. Deamidation accelerates amyloid formation and alters amylin fiber structure. *J. Am. Chem. Soc.* **2012**, *134* (30), 12658–12667.
- (11) Galletti, P.; De Bonis, M. L.; Sorrentino, A.; Raimo, M.; D'Angelo, S.; Scala, I.; Andria, G.; D'Amiello, A.; Ingrosso, D.; Zappia, V. Accumulation of altered aspartyl residues in erythrocyte proteins from patients with Down's syndrome. *FEBS J.* **2007**, *274* (20), 5263–5277.
- (12) Reinhard, L.; Tidow, H.; Clausen, M. J.; Nissen, P. Na(+),K (+)-ATPase as a docking station: protein-protein complexes of the Na(+),K (+)-ATPase. *Cell. Mol. Life Sci.* **2013**, *70* (2), 205–222.
- (13) McGrail, K. M.; Phillips, J. M.; Sweadner, K. J. Immunofluorescent localization of three Na,K-ATPase isozymes in the rat central nervous system: both neurons and glia can express more than one Na,K-ATPase. *J. Neurosci.* **1991**, *11* (2), 381–391.
- (14) Bottger, P.; Tracz, Z.; Heuck, A.; Nissen, P.; Romero-Ramos, M.; Lykke-Hartmann, K. Distribution of Na/K-ATPase alpha 3 isoform, a sodium-potassium P-type pump associated with rapid-onset of dystonia parkinsonism (RDP) in the adult mouse brain. *J. Comp. Neurol.* **2011**, *519* (2), 376–404.
- (15) Moseley, A. E.; Williams, M. T.; Schaefer, T. L.; Bohanan, C. S.; Neumann, J. C.; Behbehani, M. M.; Vorhees, C. V.; Lingrel, J. B. Deficiency in Na,K-ATPase alpha isoform genes alters spatial learning, motor activity, and anxiety in mice. *J. Neurosci.* **2007**, *27* (3), 616–626.
- (16) Medina, J. H.; Izquierdo, I. Retrograde messengers, long-term potentiation and memory. *Brain Res. Rev.* **1995**, *21* (2), 185–194.
- (17) Morris, R. G. Long-term potentiation and memory. *Philos. Trans. R. Soc., B* **2003**, *358* (1432), 643–647.
- (18) Roman, G. C.; Tatemoni, T. K.; Erkinjuntti, T.; Cummings, J. L.; Masdeu, J. C.; Garcia, J. H.; Amaducci, L.; Orgogozo, J. M.; Brun, A.; Hofman, A.; et al. Vascular dementia: diagnostic criteria for research studies. Report of the NINDS-AIREN International Workshop. *Neurology* **1993**, *43* (2), 250–260.
- (19) Kalaria, R. N.; Kenny, R. A.; Ballard, C. G.; Perry, R.; Ince, P.; Polvikoski, T. Towards defining the neuropathological substrates of vascular dementia. *J. Neurol. Sci.* **2004**, *226* (1–2), 75–80.
- (20) Braak, H.; Braak, E. Neuropathological staging of Alzheimer-related changes. *Acta Neuropathol.* **1991**, *82* (4), 239–259.
- (21) Folstein, M. F.; Folstein, S. E.; McHugh, P. R. "Mini-mental state". A practical method for grading the cognitive state of patients for the clinician. *J. Psychiatr. Res.* **1975**, *12* (3), 189–198.
- (22) Allan, L. M.; Rowan, E. N.; Firbank, M. J.; Thomas, A. J.; Parry, S. W.; Polvikoski, T. M.; O'Brien, J. T.; Kalaria, R. N. Long term incidence of dementia, predictors of mortality and pathological diagnosis in older stroke survivors. *Brain* **2011**, *134* (Pt 12), 3716–3727.
- (23) Chee, S. G.; Poh, K. C.; Trong, K. P.; Wright, P. C. Technical, experimental, and biological variations in isobaric tags for relative and absolute quantitation (iTRAQ). *J. Proteome Res.* **2007**, *6* (2), 821–827.
- (24) Evans, C.; Noirel, J.; Ow, S. Y.; Salim, M.; Pereira-Medrano, A. G.; Couto, N.; Pandhal, J.; Smith, D.; Pham, T. K.; Karunakaran, E.; Zou, X.; Biggs, C. A.; Wright, P. C. An insight into iTRAQ: Where do we stand now? *Anal. Bioanal. Chem.* **2012**, *404* (4), 1011–1027.
- (25) Wiese, S.; Reidegeld, K. A.; Meyer, H. E.; Warscheid, B. Protein labeling by iTRAQ: A new tool for quantitative mass spectrometry in proteome research. *Proteomics* **2007**, *7* (3), 340–350.
- (26) Karp, N. A.; Huber, W.; Sadowski, P. G.; Charles, P. D.; Hester, S. V.; Lilley, K. S. Addressing accuracy and precision issues in iTRAQ quantitation. *Mol. Cell. Proteomics* **2010**, *9* (9), 1885–1897.
- (27) Pichler, P.; Köcher, T.; Holzmann, J.; Mazanek, M.; Taus, T.; Ammerer, G.; Mechtler, K. Peptide labeling with isobaric tags yields higher identification rates using iTRAQ 4-plex compared to TMT 6-plex and iTRAQ 8-plex on LTQ orbitrap. *Anal. Chem.* **2010**, *82* (15), 6549–6558.

- (28) Pottiez, G.; Wiederin, J.; Fox, H. S.; Ciborowski, P. Comparison of 4-plex to 8-plex iTRAQ quantitative measurements of proteins in human plasma samples. *J. Proteome Res.* **2012**, *11* (7), 3774–3781.
- (29) Mahoney, D. W.; Therneau, T. M.; Heppelmann, C. J.; Higgins, L.; Benson, L. M.; Zenka, R. M.; Jagtap, P.; Nelsestuen, G. L.; Bergen, H. R.; Oberg, A. L. Relative quantification: Characterization of bias, variability and fold changes in mass spectrometry data from iTRAQ-labeled peptides. *J. Proteome Res.* **2011**, *10* (9), 4325–4333.
- (30) Hao, P.; Guo, T.; Li, X.; Adav, S. S.; Yang, J.; Wei, M.; Sze, S. K. Novel application of electrostatic repulsion-hydrophilic interaction chromatography (ERLIC) in shotgun proteomics: comprehensive profiling of rat kidney proteome. *J. Proteome Res.* **2010**, *9* (7), 3520–3526.
- (31) Hao, P.; Ren, Y.; Alpert, A. J.; Siu, K. S. Detection, evaluation and minimization of nonenzymatic deamidation in proteomic sample preparation. *Mol. Cell. Proteomics* **2011**, *10* (10), O111.009381.
- (32) Robinson, N. E.; Lampi, K. J.; McIver, R. T.; Williams, R. H.; Muster, W. C.; Kruppa, G.; Robinson, A. B. Quantitative measurement of deamidation in lens β B2-Crystallin and peptides by direct electrospray injection and fragmentation in a Fourier transform mass spectrometer. *Mol. Vision* **2005**, *11*, 1211–1219.
- (33) Robinson, N. E.; Robinson, A. B. Deamidation of human proteins. *Proc. Natl. Acad. Sci. U. S. A.* **2001**, *98* (22), 12409–12413.
- (34) Robinson, N. E.; Robinson, A. B. Prediction of protein deamidation rates from primary and three-dimensional structure. *Proc. Natl. Acad. Sci. U. S. A.* **2001**, *98* (8), 4367–4372.
- (35) Robinson, N. E.; Robinson, A. B. Amide molecular clocks in drosophila proteins: Potential regulators of aging and other processes. *Mech. Ageing Dev.* **2004**, *125* (4), 259–267.
- (36) Sampson, M. J.; Lovell, R. S.; Craigen, W. J. Isolation, characterization, and mapping of two mouse mitochondrial voltage-dependent anion channel isoforms. *Genomics* **1996**, *33* (2), 283–288.
- (37) Ferrer, I. Altered mitochondria, energy metabolism, voltage-dependent anion channel, and lipid rafts converge to exhaust neurons in Alzheimer's disease. *J. Bioenerg. Biomembr.* **2009**, *41* (5), 425–431.
- (38) Woltjer, R. L.; Duerson, K.; Fullmer, J. M.; Mookherjee, P.; Ryan, A. M.; Montine, T. J.; Kaye, J. A.; Quinn, J. F.; Silbert, L.; Erten-Lyons, D.; Leverenz, J. B.; Bird, T. D.; Pow, D. V.; Tanaka, K.; Watson, G. S.; Cook, D. G. Aberrant detergent-insoluble excitatory amino acid transporter 2 accumulates in Alzheimer disease. *J. Neuropathol. Exp. Neurol.* **2010**, *69* (7), 667–676.
- (39) Kirvell, S. L.; Elliott, M. S.; Kalaria, R. N.; Hortobagyi, T.; Ballard, C. G.; Francis, P. T. Vesicular glutamate transporter and cognition in stroke: a case-control autopsy study. *Neurology* **2010**, *75* (20), 1803–1809.
- (40) Nakagawa, T.; Kaneko, S. Slc1 glutamate transporters and diseases: Psychiatric diseases and pathological pain. *Curr. Mol. Pharmacol.* **2013**, *6* (2), 66–73.
- (41) Beart, P. M.; O'Shea, R. D. Transporters for L-glutamate: an update on their molecular pharmacology and pathological involvement. *Br. J. Pharmacol.* **2007**, *150* (1), 5–17.
- (42) Maragakis, N. J.; Rothstein, J. D. Glutamate transporters: animal models to neurologic disease. *Neurobiol. Dis.* **2004**, *15* (3), 461–473.
- (43) Robinson, N. E. Protein deamidation. *Proc. Natl. Acad. Sci. U. S. A.* **2002**, *99* (8), 5283–5288.
- (44) Robinson, N. E.; Robinson, A. B. Prediction of primary structure deamidation rates of asparaginyl and glutaminyl peptides through steric and catalytic effects. *J. Pept. Res.* **2004**, *63* (5), 437–448.
- (45) Robinson, N. E.; Robinson, A. B.; Merrifield, R. B. Mass spectrometric evaluation of synthetic peptides as primary structure models for peptide and protein deamidation. *J. Pept. Res.* **2001**, *57* (6), 483–493.
- (46) Robinson, N. E.; Robinson, Z. W.; Robinson, B. R.; Robinson, A. L.; Robinson, J. A.; Robinson, M. L.; Robinson, A. B. Structure-dependent nonenzymatic deamidation of glutaminyl and asparaginyl pentapeptides. *J. Pept. Res.* **2004**, *63* (5), 426–436.
- (47) Sheeley, S. A.; Kelley, W. P.; Li, L.; Sweedler, J. V. Peptide post-translational modifications affected by the MALDI-TOF measurement process. Proceedings 50th ASMS Conference on Mass Spectrometry and Allied Topics. 2002, Orlando, FL; United States. 365–366.
- (48) Kourie, J. I.; Farrelly, P. V.; Henry, C. L. Channel activity of deamidated isoforms of prion protein fragment 106–126 in planar lipid bilayers. *J. Neurosci. Res.* **2001**, *66* (2), 214–220.
- (49) Pedersen, P. A.; Jorgensen, J. R.; Jorgensen, P. L. Importance of conserved alpha -subunit segment 709GDGVND for Mg²⁺ binding, phosphorylation, and energy transduction in Na,K-ATPase. *J. Biol. Chem.* **2000**, *275* (48), 37588–37595.
- (50) Toustrup-Jensen, M.; Vilse, B. Importance of conserved Thr214 in domain A of the Na⁺,K⁺ -ATPase for stabilization of the phosphoryl transition state complex in E2P dephosphorylation. *J. Biol. Chem.* **2003**, *278* (13), 11402–11410.
- (51) Patchornik, G.; Goldshleger, R.; Karlish, S. J. The complex ATP-Fe(2+) serves as a specific affinity cleavage reagent in ATP-Mg(2+) sites of Na,K-ATPase: altered ligation of Fe(2+) (Mg(2+)) ions accompanies the E(1)→E(2) conformational change. *Proc. Natl. Acad. Sci. U. S. A.* **2000**, *97* (22), 11954–11959.
- (52) Goldshleger, R.; Patchornik, G.; Shimon, M. B.; Tal, D. M.; Post, R. L.; Karlish, S. J. Structural organization and energy transduction mechanism of Na⁺,K⁺-ATPase studied with transition metal-catalyzed oxidative cleavage. *J. Bioenerg. Biomembr.* **2001**, *33* (5), 387–399.
- (53) Faller, L. D. Mechanistic studies of sodium pump. *Arch. Biochem. Biophys.* **2008**, *476* (1), 12–21.
- (54) MacLaren, D. C.; O'Connor, C. M.; Xia, Y. R.; Mehrabian, M.; Klisak, I.; Sparkes, R. S.; Clarke, S.; Lusis, A. J. The L-isoaspartyl/D-aspartyl protein methyltransferase gene (PCMT1) maps to human chromosome 6q22.3–6q24 and the syntenic region of mouse chromosome 10. *Genomics* **1992**, *14* (4), 852–856.
- (55) Yamamoto, A.; Takagi, H.; Kitamura, D.; Tatsuoka, H.; Nakano, H.; Kawano, H.; Kuroyanagi, H.; Yahagi, Y.; Kobayashi, S.; Koizumi, K.; Sakai, T.; Saito, K.; Chiba, T.; Kawamura, K.; Suzuki, K.; Watanabe, T.; Mori, H.; Shirasawa, T. Deficiency in protein L-isoaspartyl methyltransferase results in a fatal progressive epilepsy. *J. Neurosci.* **1998**, *18* (6), 2063–2074.
- (56) McFadden, P. N.; Clarke, S. Conversion of isoaspartyl peptides to normal peptides: implications for the cellular repair of damaged proteins. *Proc. Natl. Acad. Sci. U. S. A.* **1987**, *84* (9), 2595–2599.
- (57) Kosugi, S.; Furuchi, T.; Katane, M.; Sekine, M.; Shirasawa, T.; Homma, H. Suppression of protein L-isoaspartyl (D-aspartyl) methyltransferase results in hyperactivation of EGF-stimulated MEK-ERK signaling in cultured mammalian cells. *Biochem. Biophys. Res. Commun.* **2008**, *371* (1), 22–27.
- (58) Noebels, J. L. Single-gene models of epilepsy. *Adv. Neurol.* **1999**, *79*, 227–238.
- (59) Noebels, J. L. Targeting epilepsy genes. *Neuron* **1996**, *16* (2), 241–244.
- (60) Kim, E.; Lowenson, J. D.; MacLaren, D. C.; Clarke, S.; Young, S. G. Deficiency of a protein-repair enzyme results in the accumulation of altered proteins, retardation of growth, and fatal seizures in mice. *Proc. Natl. Acad. Sci. U. S. A.* **1997**, *94* (12), 6132–6137.
- (61) Brennan, T. V.; Anderson, J. W.; Jia, Z.; Waygood, E. B.; Clarke, S. Repair of spontaneously deamidated HPr phosphocarrier protein catalyzed by the L-isoaspartate-(D-aspartate) O-methyltransferase. *J. Biol. Chem.* **1994**, *269* (40), 24586–24595.
- (62) Lowenson, J. D.; Clarke, S. Recognition of D-aspartyl residues in polypeptides by the erythrocyte L-isoaspartyl/D-aspartyl protein methyltransferase. Implications for the repair hypothesis. *J. Biol. Chem.* **1992**, *267* (9), 5985–5995.
- (63) Vatta, M.; Pena, C.; Fernandez, B. E.; Rodriguez de Lores Arnaiz, G. Endobain E, a brain Na⁺, K⁺ -ATPase inhibitor, decreases norepinephrine uptake in rat hypothalamus. *Life Sci.* **2004**, *76* (4), 359–365.
- (64) Steffens, M.; Feuerstein, T. J. Receptor-independent depression of DA and 5-HT uptake by cannabinoids in rat neocortex—Involvement of Na(+)/K(+)-ATPase. *Neurochem. Int.* **2004**, *44* (7), 529–538.
- (65) Blasi, J. M.; Cena, V.; Gonzalez-Garcia, C.; Marsal, J.; Solsona, C. Ouabain induces acetylcholine release from pure cholinergic

synaptosomes independently of extracellular calcium concentration. *Neurochem. Res.* **1988**, *13* (11), 1035–1041.

(66) Zhan, H.; Tada, T.; Nakazato, F.; Tanaka, Y.; Hongo, K. Spatial learning transiently disturbed by intraventricular administration of ouabain. *Neurol. Res.* **2004**, *26* (1), 35–40.

(67) Shinoda, T.; Ogawa, H.; Cornelius, F.; Toyoshima, C. Crystal structure of the sodium-potassium pump at 2.4 Å resolution. *Nature* **2009**, *459* (7245), 446–450.

(68) Nyblom, M.; Poulsen, H.; Gourdon, P.; Reinhard, L.; Andersson, M.; Lindahl, E.; Fedosova, N.; Nissen, P. Crystal Structure of Na⁺, K⁺-ATPase in the Na⁺-Bound State. *Science* **2013**, *342* (6154), 123–127.

(69) Kuhlbrandt, W. Biology, structure and mechanism of P-type ATPases. *Nat. Rev. Mol. Cell Biol.* **2004**, *5* (4), 282–295.